Catalysis Today 170 (2011) 148–154

Contents lists available at ScienceDirect

Catalysis Today

journal homepage: www.elsevier.com/locate/cattod

Improvements in direct borohydride fuel cells using three-dimensional electrodes

C. Ponce de León*, A. Kulak**, S. Williams, I. Merino-Jiménez, F.C. Walsh

Energy Group, Electrochemical Engineering Laboratory, School of Engineering Sciences, University of Southampton, Highfield Rd., Southampton, Hampshire SO17 1BJ, UK

ARTICLE INFO

Article history:
Received 31 October 2010
Received in revised form 2 March 2011
Accepted 3 March 2011
Available online 3 April 2011

Keywords:
Borohydride oxidation
Gold-coated reticulated vitreous carbon (RVC)
Kinetic rates constant
Porous electrode
Silver porous sponge

ABSTRACT

The oxidation of borohydride ions on three-dimensional electrodes such as vitreous carbon (RVC) coated with gold nanoparticles and silver porous sponge material was investigated. The RVC electrodes were covered with gold using PVD sputtering for different times of exposure. The open pore silver sponge electrode was prepared by the calcination of dextran or starch polymers, used as a framework, and silver nitrate mixtures between 400 and 600 °C. The porous silver was characterised by Scanning Electron Microscopy (SEM) and showed pore sizes between 1 and 20 μm. The activity of these electrodes as anode catalysts for the direct oxidation of borohydride was evaluated by cyclic voltammetry in 0.02 mol dm^{-3} $NaBH_4$ plus 3 mol dm^{-3} NaOH. The number electrons, the charge transfer coefficient and the homogeneous and kinetic rate constants were calculated and the values are comparable with those reported in the literature.

1. Introduction

As the impact of fossil fuel combustion on the climate becomes apparent, the search for renewable, efficient, clean and safe energy sources free from green gases is increasingly important. One of the possibilities for complying with these requirements is to use fuel cells as a source of energy. Fuel cells are poised to play a significant role in power generation for stationary applications, transportation and portable electronic devices. The H_2/O_2 fuel cell has been the most widely studied system but there are still concerns about the safety and efficiency aspects of transporting and storing hydrogen gas; other fuels which are safer to store and more readily available have been proposed. One of them, sodium borohydride, can be directly oxidised in combination with the reduction of oxygen in a fuel cell with a predicted specific energy of 9.3 kW h kg^{-1} which is significantly larger than other fuel cells: H_2/O_2 (0.45 kW h kg^{-1} at 4500 psi) and CH_3OH/O_2 (6.2 kW h kg^{-1}). Although these predicted energies cannot yet be reached in practice, as a number of inefficiencies still need to be resolved, they provide a guide to the most promising systems.

Over 150 papers and reviews, highlighting the most important technological advances and challenges needed to improve the performance of the direct borohydride fuel cells (DBFCs) have been published [1–4]. In its solid form, sodium borohydride absorbs water from the air and hydrolyses to form a dehydrated complex which decomposes into hydrogen gas and sodium metaborate following a pseudo first-order kinetic reaction. In aqueous solution its stability increases logarithmically with the pH, and its half life time is approximately 430 days at pH 14. The main uses as a 30 wt.% aqueous solution includes: a reducing agent in the pulp and paper industry and in the electrosynthesis of organic compounds and in waste treatment processes. The product from the oxidation, metaborate, is environmentally acceptable and can potentially be recycled to sodium borohydride [5].

1.1. Catalyst selection

The direct borohydride fuel cell (DBFC) commonly uses an air or oxygen breathing cathode and sometimes hydrogen peroxide for anaerobic applications. The attraction of the latter is its predicted specific energy of 17 kW h kg^{-1}. In the indirect borohydride fuel cell (IBFC), a catalyst is used to produce clean hydrogen gas from the hydrolysis of $NaBH_4$ which is then feed into a traditional H_2/O_2 fuel cell. These systems have been commercialised and can deliver up to 0.6 kW h kg^{-1} specific energy but are still expensive [6]. It is envisaged that the use of the direct oxidation of the BH_4^- ion on the electrode surface, rather its use as a hydrogen gas generator, can potentially deliver higher specific energy and therefore great amount of effort has been dedicated to improve the oxidation reaction and reduce its hydrolysis. This requires an anode catalyst, able to extract the predicted eight electrons from the oxidation reaction,

* Corresponding author.
** Co-Corresponding author.
E-mail address: capla@soton.ac.uk (C. Ponce de León).

0920-5861/$ – see front matter © 2011 Elsevier B.V. All rights reserved.
doi:10.1016/j.cattod.2011.03.010

carried out in strong alkaline solutions:

$$BH_4^- + 8OH^- \rightarrow BO_2^- + 6H_2O + 8e^- \qquad E^\circ = -1.24\,V\,vs.SHE \tag{1}$$

Combined with the reduction of O_2 (E° = 0.401 V *vs.* SHE) the predicted thermodynamic standard cell voltage (E^o_{cell}) for the following reaction is 1.64 V:

$$BH_4^- + 2O_2 \rightarrow BO_2^- + 2H_2O \quad E^o_{cell} = 1.64\,V \tag{2}$$

An ideal anode catalyst for borohydride would be active towards the oxidation reaction but not to the decomposition of borohydride through the hydrolysis reaction. There has been particular interest in the use of precious metals such as Au and Ag as the catalyst due to the fact that they show little catalytic activity towards the hydrolysis reaction. The number of electrons released per BH_4^- ion using gold and silver electrodes can be up to 7.5 in comparison to platinum which yielded only 4 electrons per ion [7]. Some authors however, have shown that higher number of electrons can be obtained with platinum electrodes and that there is a dependence with the concentration of borohydride; 3 and 6 electron transfer have been observed for 1 and 10 mol dm^{-3} solutions, respectively [8]. The same authors also concluded that in a silver rich AgPt alloy, silver promotes the direct oxidation of borohydride while platinum helps to increase the reaction rate. Other studies suggest that despite gold been recognised as the only catalyst that can yield the theoretical 8 electrons, platinum outperforms gold as it increases the open circuit potential (OCP), can yield 7 electrons and does not catalyse the hydrolysis of BH_4^- until nearly +0.1 V *vs.* Ag/AgCl [9]. Hydrogen evolution suppressors such as thiourea [10] and different anode compositions have been reported to improve the efficiency of the direct oxidation of borohydride. The drawback of these procedures is that the performance of the fuel cell can decrease dramatically [11].

1.2. Three dimensional electrodes

Most studies on the direct oxidation of borohydride ions have been reported using microstructures where the gold catalyst or other electroactive material is supported on carbon powder, or on solid two-dimensional electrodes. This fact limits the space-time yield of the fuel cell which could be improved by the use of three-dimensional porous electrodes. Typically, three-dimensional electrode materials used in electrochemistry include reticulated structures such as copper [12], nickel [13], aluminium [14], and reticulated vitreous carbon (RVC) [15]. Due to its low cost, high conductivity, light weight and wide selection of porosities, RVC has been widely used in electrochemical processes such as; metal recovery [16,17], sensors [18], organic synthesis [19,20], hydrogen peroxide production for the removal of organic compounds [21] and batteries and fuel cells [22,23].

In this paper we focus on the use of three-dimensional electrodes for the oxidation of borohydride ions, namely: gold-coated RVC of different pores per inch (grade ppi) and a novel silver sponge material with a three-dimensional structure. The use of three-dimensional electrodes for the direct oxidation of borohydride constitutes a novel approach that could potentially maximise the amount of borohydride ions being oxidised per unit volume in a fuel cell and consequently improve the power output of the cell.

2. Experimental details

A typical three-electrode electrochemical cell, shown in Fig. 1, was used with 0.020 mol dm^{-3} $NaBH_4$ in 3 mol dm^{-3} NaOH. All solutions were freshly prepared before the experiments. The counter electrode was a platinum mesh of 0.5 cm × 0.5 cm dimensions kept in a separate compartment divided by a cation-conducting Nafion® membrane (DuPont, NF115/H^+) to avoid the decomposition of the borohydride ions. A saturated calomel electrode (SCE) was used as a reference, connected to the working electrode compartment via a Luggin capillary positioned close to the surface of the working electrodes. A planar gold solid electrode of 0.125 cm^2 geometrical area was used to compare the electrode potentials of the oxidation of borohydride with the three dimensional electrodes. This electrode was wet polished with aqueous slurries containing decreasing sizes of alumina down to particle size of 0.1 μm. All solutions were prepared using Analytical Reagent grade from Alfa Aesar (UK) and Sigma Aldrich (Germany), and ultra-pure water (18 MΩ cm resistivity) from an Elga water purification system. Cyclic voltammetry (CV) experiments were carried out between −1.0 and +0.5 V *vs.* SCE at potential sweep rates between 20 and 200 mV s^{-1} using an EcoChemie Autolab (PGSTAT20) computer controlled potentiostat with a General Purpose Electrochemical Software (GPES) Version 4.5.

2.1. Three-dimensional working electrodes

Reticulated vitreous carbon working electrodes of 10, 20, 30, 45, 60, 80 and 100 ppi of 1.0 cm × 0.5 cm and 0.5 cm thickness were gold-coated by physical vapour deposition (PVD) using an Anatech sputtering system model Hummer® 6.2 15 mA and 8.5 kV in vacuum. The RVC material was coated on both sides during 1, 2 and 3 min, producing three electrodes per ppi grade. The silver sponge electrode was prepared using a sacrificial soft material such as starch or dextran as a template. The polymer was dissolved in concentrated silver nitrate solution and formed a viscous liquid [24]. Typically, 0.03 dm^{-3} of water were mixed with 10 g of starch or dextran and 5 g of $AgNO_3$. After solidification of this mixture at room temperature, the resulting solid was left in the furnace increasing the temperature at a rate of 0.5 °C min^{-1} to reach between 400 and 600 °C in order to calcinate the sample and remove all the organic material. The resulting structure was a silver flexible monolith with good structural properties. The self-supported macroporous silver foam exhibits a surface area of around 0.5 m^2 g^{-1} and was cut to form a three-dimensional electrode of the same dimensions as the RVC electrodes, i.e. 1.0 cm × 0.5 cm and 0.5 cm thicknesses.

3. Results and discussion

3.1. RVC electrodes

Fig. 2 shows typical current *vs.* potential curves obtained during the oxidation of borohydride ions at a concentration of 0.02 mol dm^{-3} on a gold-coated 10 ppi RVC electrode during 1 min at different potential sweep rates. The figure also shows the current density *vs.* potential of the oxidation of borohydride on a solid gold electrode with an electrode area of 0.125 cm^2 at the same electrolyte conditions and at 20 mV s^{-1} potential sweep rate. In addition, the figure shows two curves at a potential sweep rate 150 mV s^{-1} using 10 ppi RVC electrodes; one gold-coated and one uncoated. The uncoated RVC electrode was tested in the presence of borohydride and no current was observed. The gold coated electrode was tested in the absence of borohydride ions and no current was observed. The fact that these two electrodes do not produce any current indicates that the bare RVC is not active towards the oxidation of borohydride and that the electrochemical activity of the gold-coated RVC is due to the gold nanoparticles. For simplicity, only the anodic scan is shown for all curves.

Similar current *vs.* potential curves (not shown) were obtained for the 10 ppi gold-coated RVC electrodes using 2 and 3 min sputtering time. The shape of the cyclic voltammogram on the solid gold

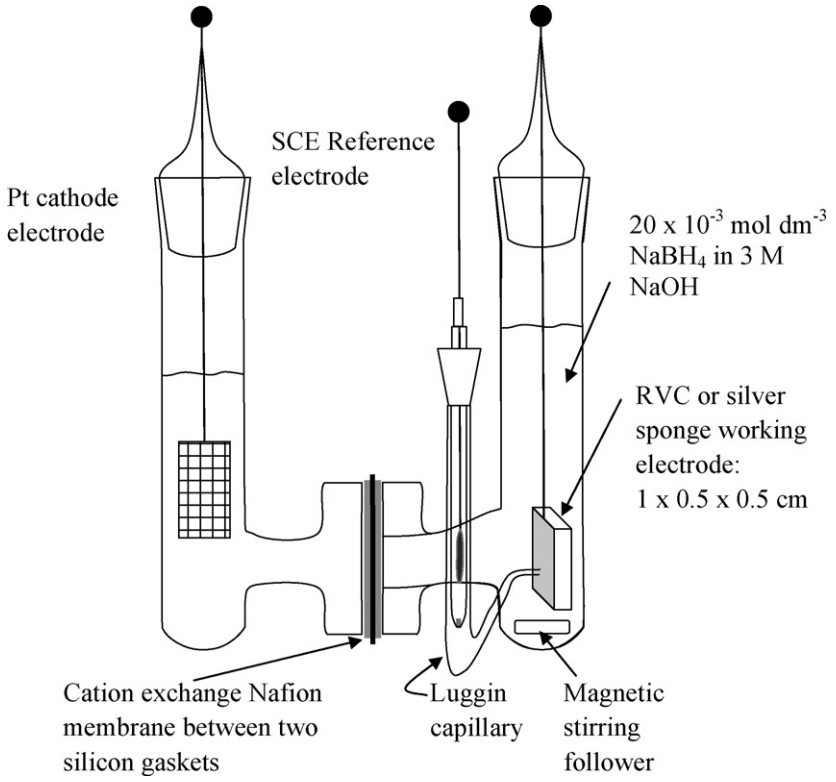

Fig. 1. Typical three-electrode cell used for the oxidation of borohydride ion at different electrodes: gold solid disc and three-dimensional electrodes: gold-coated RVC and silver sponge.

disc electrode exhibits the characteristic peak a_2 and a_3 that have been reported in the literature [25]; the first one a_2, at – 0.470 V *vs*. SCE due to the direct oxidation borohydride followed by a wide oxidation wave a_3, extending up to +0.42 V *vs*. SCE possibly due to the oxidation of intermediates. The curves for the oxidation of borohydride on the 10 ppi gold-coated RVC electrode show two peaks at a potential sweep rate of 20 mV s^{-1}; a'_2 and a'_3 at 0 V and +0.4 V *vs*. SCE, respectively. These peaks are possibly due to the same processes observed on the solid gold electrode. The potential of the oxidation peak a'_2 appears at approximately 0.470 V more positive compared with the same peak on the gold solid electrode at 20 mV s^{-1} while the oxidation of the possible intermediates, a'_3, appears at similar potential values, i.e. +0.4 V *vs.* SCE. The potential of the peak a'_2 shifts with the potential sweep rate from approximately 0 V *vs*. SCE at 20 mV s^{-1} to +0.3 V *vs*. SCE at 200 mV s^{-1}. This large potential change with the sweep rate is characteristic of the irreversible nature of the oxidation process of borohydride. The peak a'_3 also shifts slightly towards positive values and eventually becomes overlapped by the peak a'_2 in a single broad peak as the potential sweep rate increases. The curve in the absence of borohydride probes, together with the comparison with the literature that the process observed on the gold-coated RVC corresponds to the direct oxidation of borohydride ions.

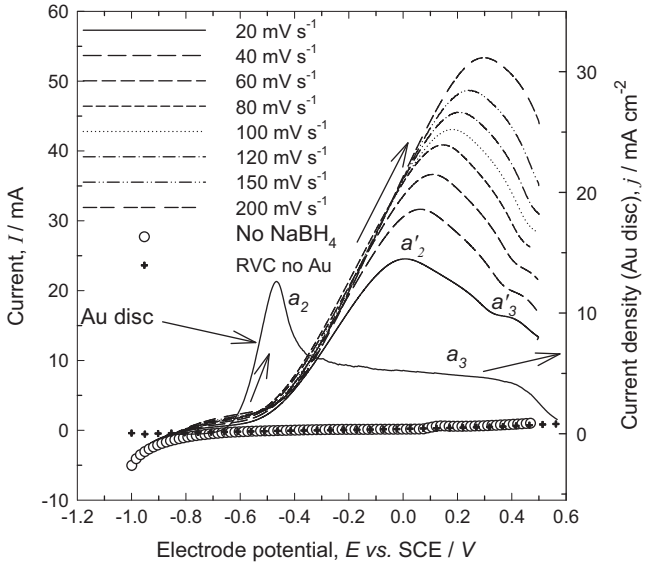

Fig. 2. Cyclic voltammograms of 0.02 mol dm^{-3} $NaBH_4$ in 3 mol dm^{-3} NaOH on a gold disc electrode (0.125 cm^2) and on a 10 ppi RVC gold-coated electrode after a coating time of one minute at different potential sweep rates and 298 K. The curves obtained in the absence of borohydride (○) and on the uncoated RVC(+) were recorded at a potential sweep rate of 200 mV s^{-1}.

During the reverse sweep potential, not shown in the figure for clarity, the curves also presented the sharp oxidation peak c'_1 [25,26], assigned to the oxidation of some intermediate products such as BH_3OH^- as reported in the literature [25]. Similar current potential curves as those shown in Fig. 2 were also obtained for the other gold-coated RVC ppi grade electrodes (20, 30, 45, 60, 80 and 100 ppi) with similar features i.e.; three oxidation peaks: a'_1, a'_2 and c'_1 where the oxidation potentials shifted towards positive values with the potential sweep rate.

The dependence of electrode potential E_p, at the peak current with the potential sweep rate can be analysed with the equation for irreversible systems assuming an electrochemical process only [26]:

$$E_p = E^o + \left\{\frac{1}{f(1-\alpha)n_a}\right\}\left\{0.78 + \ln\left(\frac{D_{BH_4^-}^{1/2}}{k_s}\right) + \ln[(1-\alpha)n_a \upsilon f]^{1/2}\right\} \quad (3)$$

where E^o is the formal electrode potential for the oxidation of borohydride, $D_{BH_4^-}$ is the diffusion coefficient, n_a is equal to 1, the number of electrons involved in the rate determining step, α the charge transfer coefficient, υ is the potential sweep rate, k_s is the heterogeneous rate constant and f (= F/RT) is a constant equal to 32.92 V^{-1}. The calculation of the mass transfer coefficient from the slopes of the E_p *vs.* $\ln \upsilon$ curves (Eq. (3)) for the gold coated RVC electrodes lies within the values of 0.87 and 0.98 for all the RVC gold coated electrodes depending on the ppi grade. The values are slightly larger than the value of 0.84 reported by Santos et al. [26] at similar conditions on a solid gold macroelectrode. This might suggest that the gold nanoparticles on the RVC electrode are more easily covered by the oxidation product of borohydride, than a larger polycrystalline gold surface, making the reaction increasingly sluggish.

Fig. 3 shows the peak current *vs.* the square root of the potential sweep rate for different gold-coated RVC ppi grades during 1 (Fig. 3a), 2 (Fig. 3b) and 3 (Fig. 3c) minutes deposition time. The general trend shows that the peak current of the oxidation process increases with the square root of the potential sweep rate however, not all the RVC electrodes exhibited linear behaviour. This was attributed to a non-uniform gold deposition process or to some defects on the RVC structure which avoided good adherence of gold on the carbon substrate. The electrodes shown in the Fig. 3 are those that presented an approximate linear behaviour. Assuming that the oxidation of borohydride ions occur in a single-step irreversible process, the following expression can be used to correlate the relationship between the peak current and the potential sweep rate [27]:

$$I_p = (3 \times 10^5)[(1-\alpha)n_a]^{1/2} n A D_{BH_4^-}^{1/2} c \upsilon^{1/2} \quad (4)$$

where I_p is the peak current, A is the geometrical surface area of the RVC electrodes, n is the total number of electrons and c is the concentration of borohydride ions. The justification to use equation (3) is based on the assumption that the very fast successive steps involved in the oxidation cannot be differentiated at the potential sweep rates used in these experiments and a single step is assumed [26]. The diffusion coefficient of borohydride ions calculated from various electrochemical techniques at 298 K is: 2.1×10^{-5} cm^2 s^{-1} from polarography studies [28], 1.6×10^{-5} cm^2 s^{-1} using Au microelectrodes [29] and variations with the temperature from $1.09 \pm 0.05 \times 10^{-5}$ cm^2 s^{-1} at 293 K to $2.36 \pm 0.07 \times 10^5$ cm^2 s^{-1} at 333 K, calculated via chronoamperometry on a spherical Au electrode [30]. Other authors have found larger values of the diffusion coefficient: 2.42×10^{-5} cm^2 s^{-1} at 298 K to 5×10^{-5} cm^2 s^{-1} at 335 K. The calculation of the number of electrons in this work was carried out by taking an average value of 2.1×10^{-5} cm^2 s^{-1} for the diffusion coefficient [28,30] and a charge transfer coefficient α, between 0.87 and 0.98, depending on the porosity grade (ppi) of the RVC electrode used. Although it has been found that gold does not necessarily yield the number of electrons predicted, many studies use the theoretical 8 electrons as an approximation; for example Santos et al. suggested 7.6 electrons transfer at 298 K and 0.03 mol dm^{-3} concentration of borohydride [26]. Other authors have reported different values depending on the oxidation potential and suggest that the value seems to be influenced by the further oxidation reaction of some intermediates which can cause superimposed currents and bring the average number of electrons lower or higher than the predicted 8 [31]. In this work the number of electrons transferred during the oxidation of borohydride on the different gold-coated RVC electrodes using Eq. (4) varies between 5.5 and 10.3. Although the average value was 8 electrons the largest values suggest superimposed currents and uneven potential and current distribution on the three dimensional electrodes.

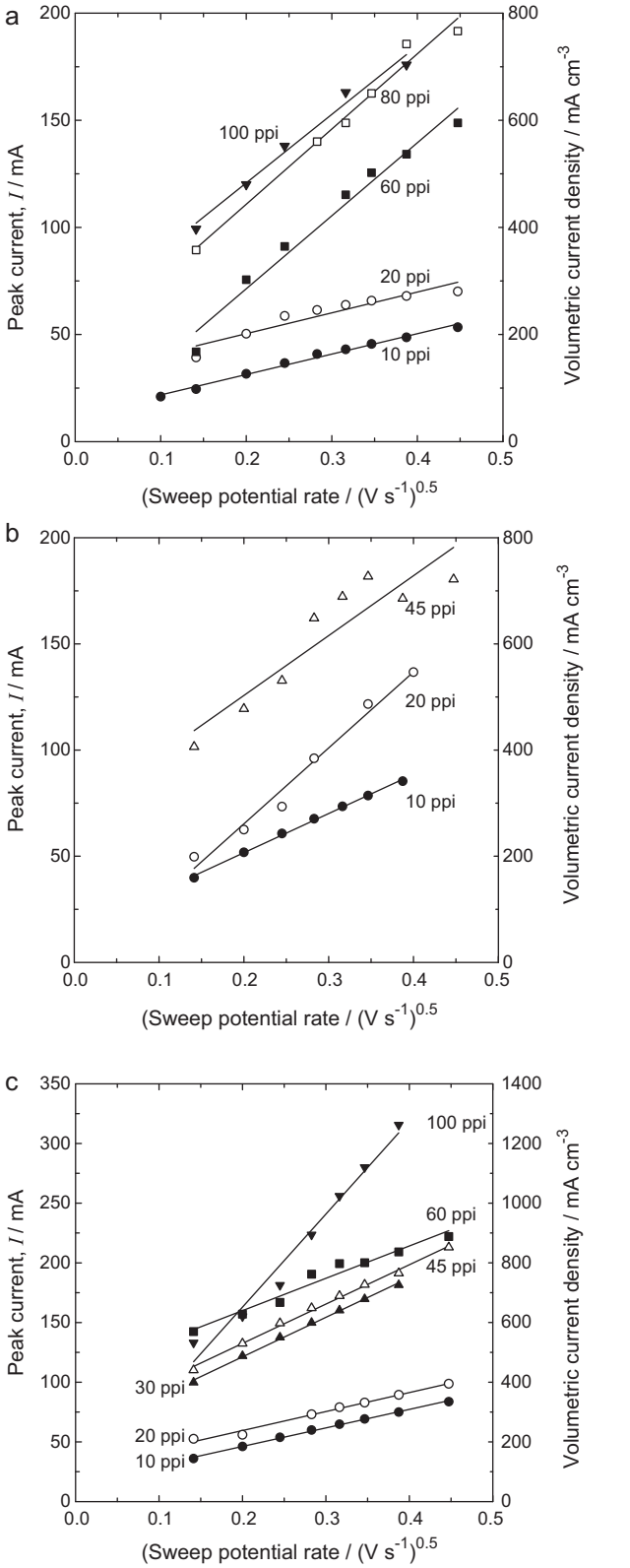

Fig. 3. Peak current I_p, *vs.* the square root of the potential sweep rate $\upsilon^{1/2}$ for the RVC gold-coated electrodes after different times of gold sputtering: (a) 1, (b) 2 and (c) 3 min, during the oxidation of borohydride ions in 0.02 mol dm^{-3} $NaBH_4$ in 3 mol dm^{-3} NaOH.

The heterogeneous rate constant of the oxidation process can be calculated using the following equation:

$$I_p = 0.227 n F A c_{BH_4^-} k_s \exp\left\{\left[\frac{(1-\alpha)n_a F}{RT}\right](E_p - E^o)\right\} \quad (5)$$

Table 1
Heterogeneous and kinetic rates constants for the different gold coated RVC electrodes and the silver sponge electrodes at 298 K. 0.02 mol dm^{-3} $NaBH_4$ in 3 mol dm^{-3} NaOH.

Porosity grade RVC	PVD deposition time/min	k_s /10^5 cm s^{-1}	Potential *vs.* SCE/V					
			−0.5	−0.3	−0.1	0.1	0.3	0.5
			Kinetic rate constant at different potentials, k/10^3 cm s^{-1}					
10 ppi	1	15	7	15	30	70	150	330
	2	7	10	30	70	200	540	1500
	3	25	7	15	25	50	100	200
20 ppi	2	15	6	15	30	60	130	270
	3	40	5	9	15	25	40	70
30 ppi	1	70	4	6	9	15	20	30
	2	60	2	3	4	6	7	10
	3	75	5	7	10	15	20	30
45 ppi	3	50	8	15	25	40	70	130
60 ppi	1	50	1	1	1	2	2	2
	3	180	7	10	15	20	20	30
80 ppi	1	40	1	1	1	1	2	2
100 ppi	1	20	0.5	1	1	1	1	1
	3	50	1	1	1	1	1	2
Ag sponge	–	9×10^{-5}	0.003	0.016	0.084	0.5	2	12

Table 1 shows the values of the rate constants for the different gold-coated RVC electrodes together with the values of the kinetic rate constants at different potentials calculated using the equation:

$$k = k_s \exp\left\{\left[\frac{(1-\alpha)n_a F}{RT}\right](E - E^o)\right\} \quad (6)$$

The values of the heterogeneous rate constant are in the order of 10^{-5} cm s^{-1} and are comparable with those obtained by cyclic voltammetry on a gold solid electrode with an area of 3.14×10^{-2} cm^{-2} [26]. However, the obtained values are two orders of magnitude lower when compared with those reported by other authors using different techniques, for example Finkelstein et al. [9] found a value of 6.8×10^{-2} cm s^{-1} using the Koutecký–Levich equation on a 5 mm Au rotating disk electrode. This could be due to the choice of the E^o value or to the blockage of the gold nanoparticles on the gold-coated RVC electrodes. Although there are some exceptions, the values of the heterogeneous rate constant tend to increase slightly with the porosity grade and the deposition time. The table also shows the dependence of the kinetic rate constant with the electrode potential. The values are in the same order of magnitude to those reported in the literature [26,31]. The general trend is that the rate constant decreases with the porosity grade of the electrode; at lower electrode potentials the difference is not significant but as the electrode potential become more positive, the difference increases, this result suggests that on lower ppi gold-coated RVC electrodes such as 10, 20 and 30 the reaction is faster than on the higher grades.

3.2. Silver foam electrode

Fig. 4a and b shows the scanning electron microscopy images of the silver sponge prepared as described in Section 2 using starch as a polymer framework. The image in Fig. 4a shows the highly porous structure of the silver foam formed after the calcination process with pore sizes between 1 and 20 μm. The sponge was mechanically firm with certain degree of flexibility and it was found that its mechanical properties were dependent on the ratio of silver nitrate to polymer used. The temperature and time of calcination also played an important role in the formation of the structure [24]; high temperatures promoted certain degree of syntherisation while at low temperatures some of the polymeric carbon could remain within the structure. Fig. 4b shows a close up of the foam where it can be seen that it is formed by randomly joined long globular strands of silver that changes diameter approximate between 2 and 7 μm, to form a highly porous material.

Fig. 5 shows the cyclic voltammograms of 0.02 mol dm^{-3} $NaBH_4$ in 3 ml dm^{-3} NaOH on the silver sponge electrode described above at potential sweep rate of 20 and 200 mV s^{-1}. The figure also shows the curve when the cyclic voltammogram was carried out in the absence of $NaBH_4$ and shows a peak at around −0.15 V *vs.* SCE when

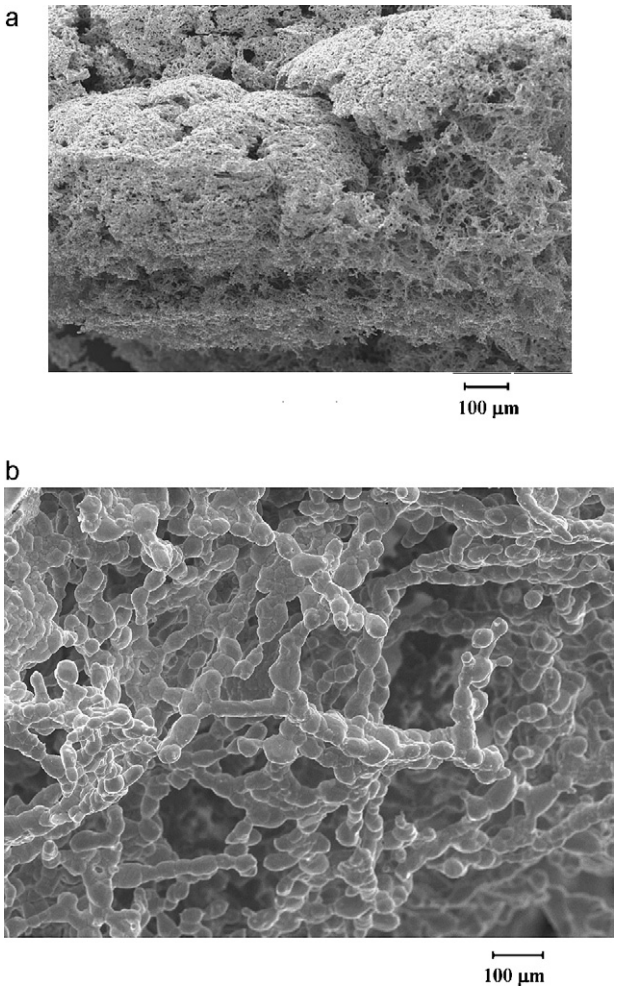

Fig. 4. Scanning electron micrographs of silver sponge: (a) bulk materials and (b) globular strands.

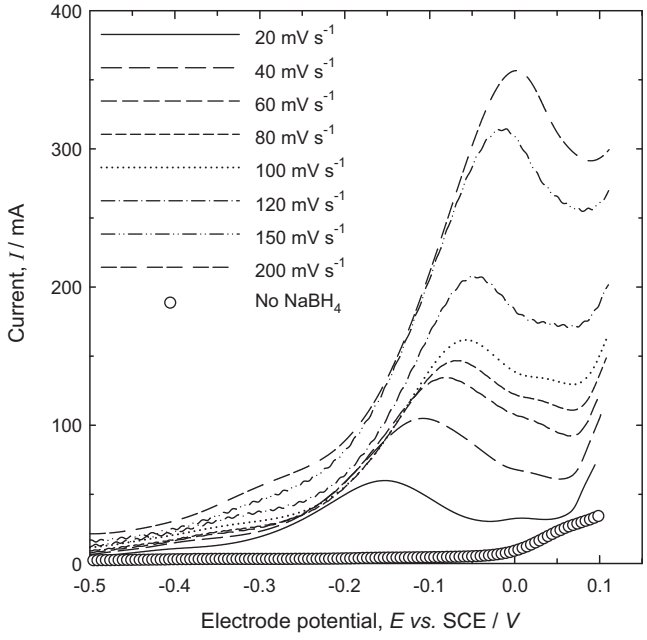

Fig. 5. Cyclic voltammograms of 0.02 mol dm^{-3} $NaBH_4$ in 3 mol dm^{-3} NaOH on a silver sponge electrode at different sweep potential rates. The dimensions of the electrode were approximately 1 cm × 0.5 cm × 0.5 cm. The curve without $NaBH_4$ was at a potential sweep rate of 150 mV s^{-1}.

the sweep potential rate was 20 mV s^{-1} is due to the direct oxidation of borohydride ions. The peak potential shifts to 0 V *vs.* SCE when the potential sweep rate was 200 mV s^{-1} according to the slow irreversible electron transfer process, characteristic of the oxidation of borohydride. The value of the potential for the oxidation of borohydride is similar to the one reported by Hernandez-Ramirez et al. [34] between −0.3 V and −0.05 V *vs.* SCE when the oxidation was carried out on a polycrystalline silver electrode. The voltammograms were reversed at 0.1 V *vs.* SCE to avoid the oxidation of silver that occurs at around 0.15 V *vs.* SCE with the formation of an Ag_2O monolayer [32] followed by bulk Ag_2O deposition and AgO at +0.25 V *vs.* SCE and +0.55 V *vs.* SCE, respectively [33,34]. The peak current of the curves shown in Fig. 5 changed linearly with the square root of the potential sweep rate as shown in Fig. 6. The figure also shows the data of peak currents *vs.* the square root of the potential sweep rate obtained for the 3 min PVD gold-coated RVC of 100 ppi grade and the 1 min gold-coated 10 ppi RVC electrodes. The 100 ppi grade RVC electrode and the silver sponge showed the highest peak currents for the oxidation of borohydride reaching up to 300 mA at 150 mV s^{-1} potential sweep rates. Using the Eqs. (3)–(5) and the same assumptions made for the gold-coated RVC electrodes the number of electrons, the charge transfer coefficient and the heterogeneous rate constant were 7.1, 0.78 and 9×10^{-10} cm s^{-1}, respectively. The values of the number of electrons transferred and the heterogeneous rate constant suggest that the oxidation reaction was efficient but with very slow start in comparison with the gold-coated RVC electrodes. Despite this, Table 1 shows towards positive potentials the oxidation reaction can be faster than on some of the high grade ppi gold-coated RVC electrodes. This electrode seems promising for the oxidation of borohydride and constitutes a viable option to increase the amount of borohydride than can be oxidised per unit volume of electrode however, needs further optimization to find out the ideal mixture polymer-silver nitrate mixture. This is currently being investigated in our laboratory.

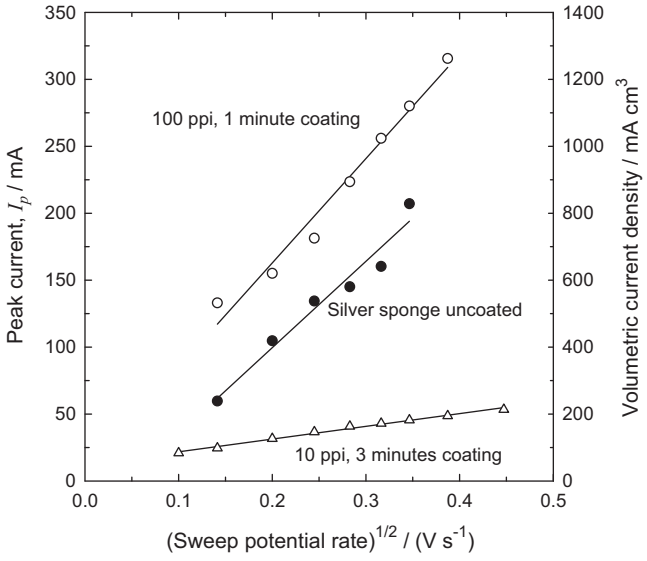

Fig. 6. Comparison of the peak current *vs.* the square root of the sweep potential rate for different electrodes of similar dimensions.

4. Conclusions

The PVD gold deposition shows that using three-dimensional electrodes is advantageous for the oxidation of borohydride. The current due to the oxidation of borohydride increases when the porosity of the gold-coated RVC electrodes increases from 10 to 100 ppi at constant deposition times. Similar situation occurs when the gold deposition time increases for the same porosity grade gold-coated RVC electrodes; the general trend is that the current due to the oxidation of borohydride increases as larger amount of gold is deposited. The value of the charge transfer coefficient on the gold-coated RVC electrodes varies between 0.87 and 0.98 depending on the ppi and the deposition time. The average number of electrons transferred was 8, but lower (e.g., 5.5) and larger (e.g., 10.3) values were also found possibly due to the uneven current and potential distribution on the three dimensional electrodes. This suggests that the thickness of the RVC electrode and coating quality should be optimised. The heterogeneous and kinetic rate constants for the oxidation of borohydride ion these electrodes are of the same order of magnitude as those reported in the literature using cyclic voltammetry however, the values are smaller than those obtained using rotating disc electrodes.

Silver sponge electrodes prepared from a calcination method of a polymer matrix and silver nitrate shows reasonable activity towards the oxidation of borohydride ions at positive potentials. The electrode potential value of the oxidation of borohydride ions on this electrode agrees with the values reported in the literature and the reaction is diffusion controlled. The optimization and a more complete characterisation of this electrode are necessary to find out the optimal mixture of polymer-silver nitrate to make all the electrode surface area available for the oxidation of borohydride.

References

[1] A.L.W. Vielstich, H.A. Gasteiger (Eds.), Handbook of Fuel Cells-Fundamentals, Technology and Applications, vol. 1–4, Wiley, 2003.
[2] G. Hoogers (Ed.), Fuel Cell Technology Handbook, CRC Press, 2003.
[3] B.H. Liu, Z.P. Li, J. Power Sources 187 (2009) 291–297.
[4] U.B. Demirci, J. Power Sources 172 (2007) 676–687.
[5] Y. Kojima, T. Haga, Int. J. Hydrogen Energy 28 (2003) 989–993.
[6] H.E. Systems, Fuel Cell Propolsion System for Unmanned Aerial Vehicles, available from: http://www.hes.sg/products.html (accessed 1.04.11).
[7] M. Chatentet, F. Micoud, I. Roche, E. Chainet, Electrochim. Acta 51 (2006) 5459–5467.
[8] B.M. Concha, M. Chatenet, Electrochim. Acta 54 (2009) 6119–6129.
[9] D.A. Finkelstein, N.D. Mota, J.L. Cohen, H.D. Abruña, J. Phys. Chem. C 113 (2009) 19700–19712.

[10] C. Celik, F.G.B. San, H.I. Sarac, Int. J. Hydrogen Energy 35 (2010) 8678–8682.
[11] R. Jamard, A. Latour, J. Salomon, P. Capron, A. Martinent-Beaumont, J. Power Sources 176 (2007) 287–292.
[12] A. Tentorio, U. Casolo-GGinelli, J. Appl. Electrochem. 8 (1978) 195–205.
[13] P. Zhao, H. Zhang, H. Zhou, B. Yi, Electrochim. Acta 51 (2005) 1091–1098.
[14] Y. Boonyongmaneerat, C.A. Schuh, D.C. Dunand, Scripta Mater. 59 (2008) 336–339.
[15] J.M. Friedrich, C. Ponce de León, G.W. Reade, F.C. Walsh, J. Electroanal. Chem. 561 (2004) 203–217.
[16] Q. de Radiguès, R. Santoro, J. Proost, Chem. Eng. J. 162 (2010) 273–277.
[17] C. Ponce de León, D. Pletcher, Electrochim. Acta 42 (1996) 533–541.
[18] P. Hrnčířová, F. Opekar, K. Šulík, Sensors Actuators B: Chem. 69 (2000) 199–204.
[19] L. Mattiello, L. Rampazo, Electrochim. Acta 42 (1997) 2257–2264.
[20] D. Szánto, P. Trinidad, F.C. Walsh, J. Appl. Electrochem. 28 (1998) 251–258.
[21] C. Ponce de León, D. Pletcher, J. Appl. Electrochem. 25 (1995) 307–314.
[22] E. Gyenge, J. Jung, B. Mahato, J. Power Sources 113 (2003) 388–395.
[23] T.T. Cheng, E.L. Gyenge, J. Appl. Electrochem. 38 (2008) 51–62.
[24] D. Walsh, L. Arcelli, T. Ikoma, J. Tanaka, S. Mann, Nat. Mater. 2 (2003) 386–390.
[25] E. Gyenge, Electrochim. Acta 49 (2004) 965–978.
[26] D.M.F. Santos, C.A.C. Sequeira, Electrochim. Acta 55 (2010) 6775–6781.
[27] D. Pletcher, A First Course in Electrode Processes, The Royal Society of Chemistry, Cambridge, 2009.
[28] J.A. Gardiner, J.W. Collat, Inorg. Chem. 4 (1965) 1208–1212.
[29] G. Denuault, M.V. Mirkin, A.J. Bard, J. Electroanal. Chem. 308 (1991) 27–38.
[30] K. Wang, J. Lu, L. Zhuang, J. Electroanal. Chem. 585 (2005) 191–196.
[31] H. Cheng, K. Scott, Electrochim. Acta 51 (2006) 3429–3433.
[32] B.M. Jovic, V.D. Jovic, J. Serb. Chem. Soc. 69 (2004) 153–166.
[33] E.R. Savinova, D. Zemlyanov, B. Pettinger, A. Scheybal, R. Schlögl, K. Doblhofer, Electrochim. Acta 46 (2000) 175–183.
[34] V.A. Hernández-Ramírez, A. Alatorre-Ordaz, M.L. Yepez-Murrieta, J.G. Ibañez, C. Ponce de León, F.C. Walsh, ECS Trans. 20 (2009) 211–225.